Electronic Supplementary Material (ESI) for Journal of Materials Chemistry C.
This journal is © The Royal Society of Chemistry 2015

SUPPORTING INFORMATION

Non-stoichiometric Compositions Arising from Synergistic Electronic and Size Effects. Syntheses, Crystal Chemistry and Electronic Properties of $A_{14}Cd_{1+x}Pn_{11}$ Compounds ($0 \leq x \leq 0.30$; A = Sr, Eu; Pn = As, Sb)

Julien P. A. Makongo, Gregory M. Darone, Sheng-Qing Xia, and Svilen Bobev[a]

Department of Chemistry and Biochemistry, University of Delaware, Newark, Delaware 19716, United States

Corresponding Author

E-mail: bobev@udel.edu. Phone: (302) 831-8720. Fax: (302) 831-6335.

Table S1. Anisotropic Displacement Parameters (Å^2) for A_{14}CdPn_{11} and (A = Sr, Eu and Pn = As, Sb); $U_{12} = U_{13} = U_{23} = 0$

Atom	Site	U_{11}	U_{22}	U_{33}
		$Sr_{14}Cd_{1.06(1)}As_{11}$		
Sr1	32*g*	0.0239(3)	0.0226(3)	0.0245(3)
Sr2	32*g*	0.0205(3)	0.0286(4)	0.0293(3)
Sr3	16*e*	0.0188(4)	0.0171(4)	0.0223(4)
Sr4	32*g*	0.0397(4)	0.0186(3)	0.0268(3)
Cd1	8*a*	0.0198(3)	0.0198(3)	0.0193(4)
As1	16*f*	0.0223(3)	0.0223(3)	0.0243(5)
As2	32*g*	0.0172(3)	0.0169(3)	0.0224(3)
As3A	32*g*	0.0305(5)	0.017(4)	0.0222(4)
As3B	32*g*	0.0305(5)	0.017(4)	0.0222(4)
As4	16*f*	0.0159(6)	0.0159(6)	0.0201(8)
		$Eu_{14}CdAs_{11}$		
Eu1	32*g*	0.0113(2)	0.011(2)	0.0122(2)
Eu2	32*g*	0.01(2)	0.0121(2)	0.0166(2)
Eu3	16*e*	0.0105(3)	0.0095(3)	0.0136(3)
Eu4	32*g*	0.0217(2)	0.0094(2)	0.0123(2)
Cd1	8*a*	0.0105(3)	0.0105(3)	0.0105(5)
As1	16*f*	0.0134(4)	0.0134(4)	0.0113(5)
As2	32*g*	0.0091(4)	0.0095(4)	0.0154(4)
As3	32*g*	0.0167(4)	0.0121(4)	0.0119(4)
As4	16*f*	0.0112(10)	0.0112(10)	0.0087(8)
		$Sr_{14}Cd_{1.30(1)}Sb_{11}$		
Sr1	32*g*	0.0178(3)	0.0203(3)	0.0181(3)
Sr2	32*g*	0.0182(3)	0.0322(4)	0.0245(3)
Sr3	16*e*	0.0121(4)	0.0132(4)	0.0134(4)
Sr4	32*g*	0.0414(4)	0.0147(3)	0.0145(3)
Cd1	8*a*	0.0165(4)	0.0165(4)	0.0142(5)
Sb1	16*f*	0.0137(2)	0.0137(2)	0.0142(3)
Sb2	32*g*	0.0141(2)	0.0127(2)	0.0188(2)
Sb3	32*g*	0.0265(2)	0.0142(2)	0.0187(2)
Sb4	8*b*	0.0429(4)	0.0429(4)	0.0148(4)
		$Eu_{14}Cd_{1.27(1)}Sb_{11}$		
Eu1	32*g*	0.0161(3)	0.0173(3)	0.0188(3)
Eu2	32*g*	0.0166(3)	0.0282(3)	0.0261(3)
Eu3	16*e*	0.0119(3)	0.0127(3)	0.0134(3)
Eu4	32*g*	0.0396(4)	0.0139(3)	0.0154(3)
Cd1	8*a*	0.0147(4)	0.0147(4)	0.016(7)
Sb1	16*f*	0.0124(3)	0.0124(3)	0.015(5)
Sb2	32*g*	0.0125(3)	0.0124(3)	0.0194(3)
Sb3	32*g*	0.0243(4)	0.0133(3)	0.0172(3)
Sb4	8*b*	0.0314(6)	0.0314(6)	0.0183(7

Table S2. Selected Crystal Data and Structure Refinement Parameters for $Sr_{14}Cd_{1.4(1)}Sb_{11}$ and synthesized by a solid state reaction in welded Nb tube.

Empirical formula	$Sr_{14}Cd_{1.4(1)}Sb_{11}$
Formula weight	2726.8
Temperature	120(2)K
Radiation, λ	Mo$K\alpha$, 0.71073 Å
Space group, Z	$I4_1/acd$ (No 142), 8
a (Å)	17.645(2)
b (Å)	17.645(2)
c (Å)	23.117(3)
V (Å^3)	7197(1)
ρ_{cal} (g/cm^3)	5.03
μ (cm^{-1})	294.6
Goodness-of-fit on F^2	0.98
R_1 ($I > 2\sigma_I$)[a]	0.037
wR_2 ($I > 2\sigma_I$)[a]	0.081
Largest diff. peak and hole (e$^-$/Å^{-3})	3.21, −3.07

[a] $R_1 = \Sigma||F_o| - |F_c||/\Sigma|F_o|$; $wR_2 = [\Sigma\,[w(F_o^2 - F_c^2)^2]/\Sigma\,[w(F_o^2)^2]]^{1/2}$, where $w = 1/[\sigma^2 F_o^2 + (0.03P)^2]$ and $P = (F_o^2 + 2F_c^2)/3$.

Table S3. Atomic Coordinates and Equivalent Isotropic Displacement Parameters (U_{eq}[a]) for $Sr_{14}Cd_{1.4(1)}Sb_{11}$

Atom	Site	x	y	z	Occupancy	U_{eq} (Å^2)
			$Sr_{14}Cd_{1.4(1)}Sb_{11}$			
Sr1	32*g*	0.04193(6)	0.07454(6)	0.1724(4)	1	0.0168(3)
Sr2	32*g*	0.02429(6)	0.37531(7)	0.00144(5)	1	0.0254(3)
Sr3	16*e*	0.35302(8)	0	1/4	1	0.0096(3)
Sr4	32*g*	0.3417(7)	0.07319(6)	0.09427(4)	1	0.0214(3)
Cd1	8*a*	0	1/4	3/8	1	0.0125(3)
Cd2[b]	32*g*	0.473(4)	0.0054(4)	0.077(3)	0.10(1)	0.007(2)
Sb1	16*f*	0.13471(3)	0.38471(4)	1/8	1	0.0108(2)
Sb2	32*g*	0.358(4)	0.25637(4)	0.06154(3)	1	0.0121(2)
Sb3	32*g*	0.12876(4)	0.02817(4)	0.04513(3)	1	0.0167(2)
Sb4	8*b*	0	1/4	1/8	1	0.0291(7)

[a] U_{eq} is defined as one-third of the trace of the orthogonalized U_{ij} tensor.
[b] Refined isotropically.

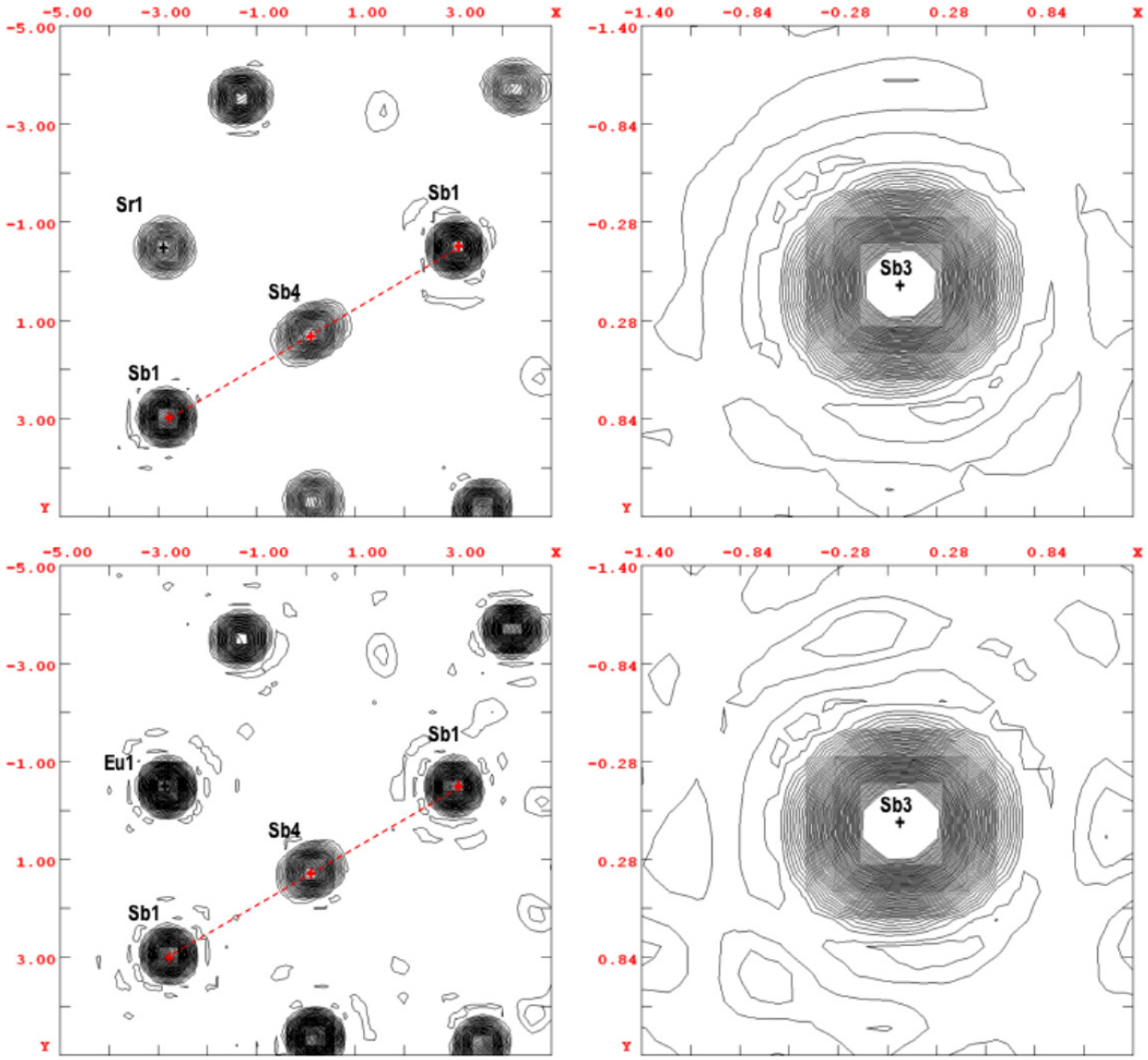

Figure S1. Two-dimensional (2D) contour plot of the observed Fourier electron density (3–6 $e^{-}/Å^3$) from the refined atomic positions showing a cigar-shaped like thermal ellipsoid for the central position (Sb4) of the linear hypervalent $[Sb_3]^{7-}$ anion (scaled in 5 × 5 Å), and a spherical shaped-like thermal ellipsoid for Sb3 (scaled in 1.4 × 1.4 Å) in the crystal structure of $Sr_{14}Cd_{1.30}Sb_{11}$ (top) and $Eu_{14}Cd_{1.27}Sb_{11}$ (bottom), respectively.

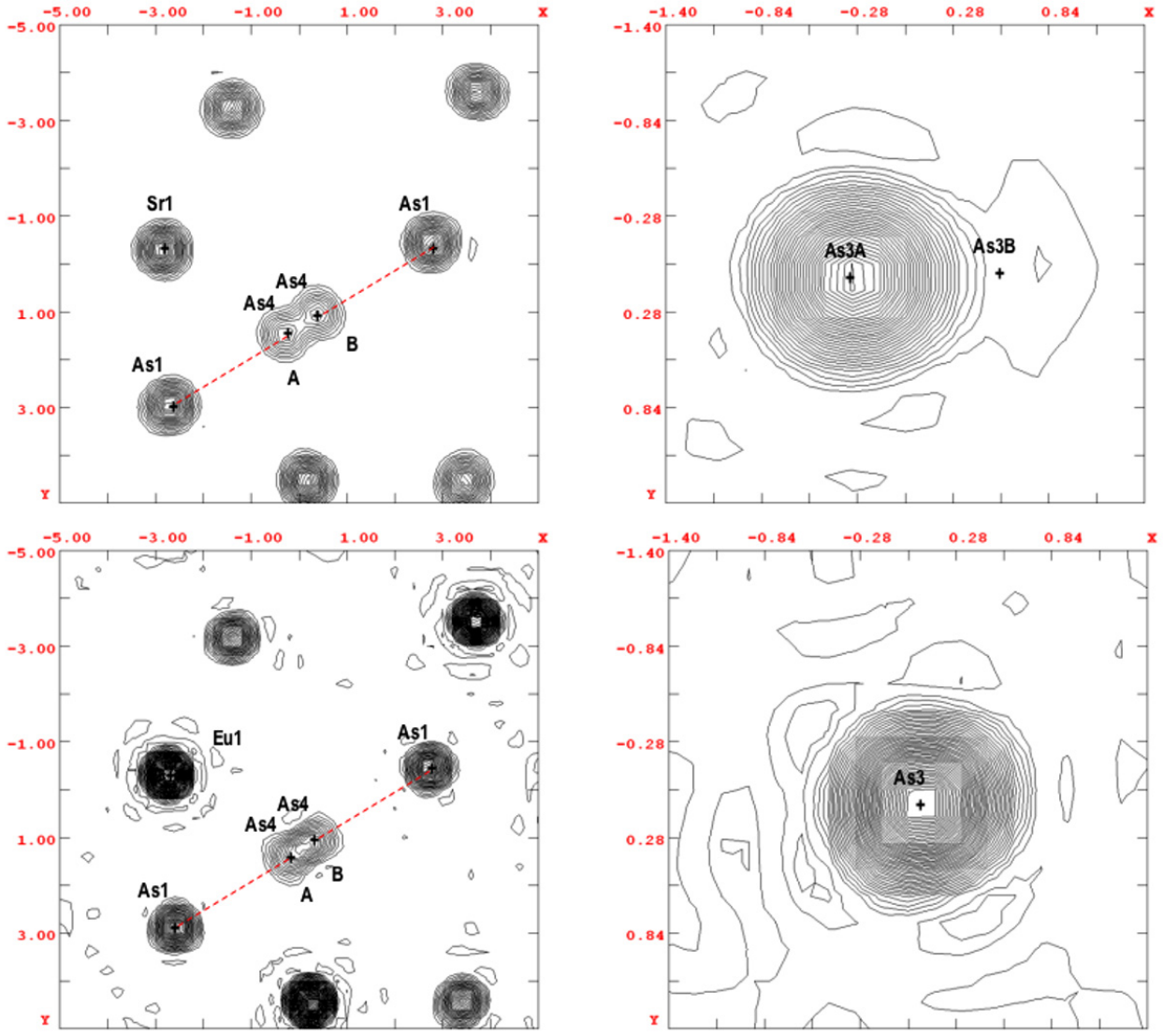

Figure S2. 2D contour plot of the observed Fourier electron density (3–6 $e^{-}/Å^{3}$) from the refined atomic positions showing a cigar-shaped like thermal ellipsoid for the central position (As4) of the linear hypervalent $[As_3]^{7-}$ anion (scaled in 5 × 5 Å), and a spherical shaped-like thermal ellipsoid for As3 (scaled in 1.4 × 1.4 Å) in the crystal structure of $Sr_{14}Cd_{1.06}As_{11}$ (top) and $Eu_{14}CdAs_{11}$ (bottom), respectively.

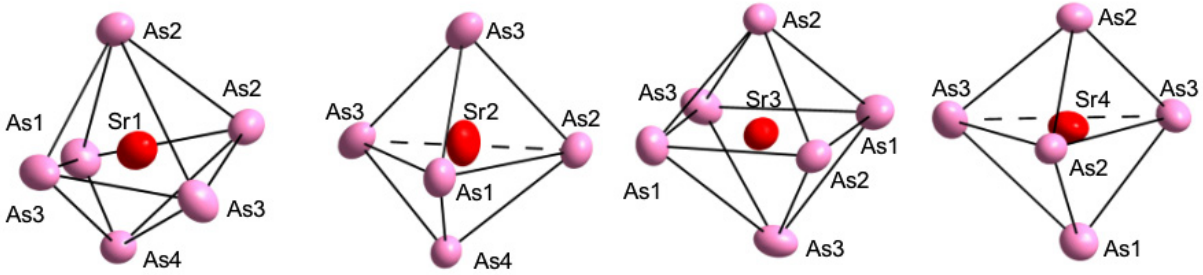

Figure S3. First coordination spheres for the cations in the "14-1-11" structure. Shown are the polyhedra for the Sr atoms in the structure of $Sr_{14}Cd_{1.06}As_{11}$.

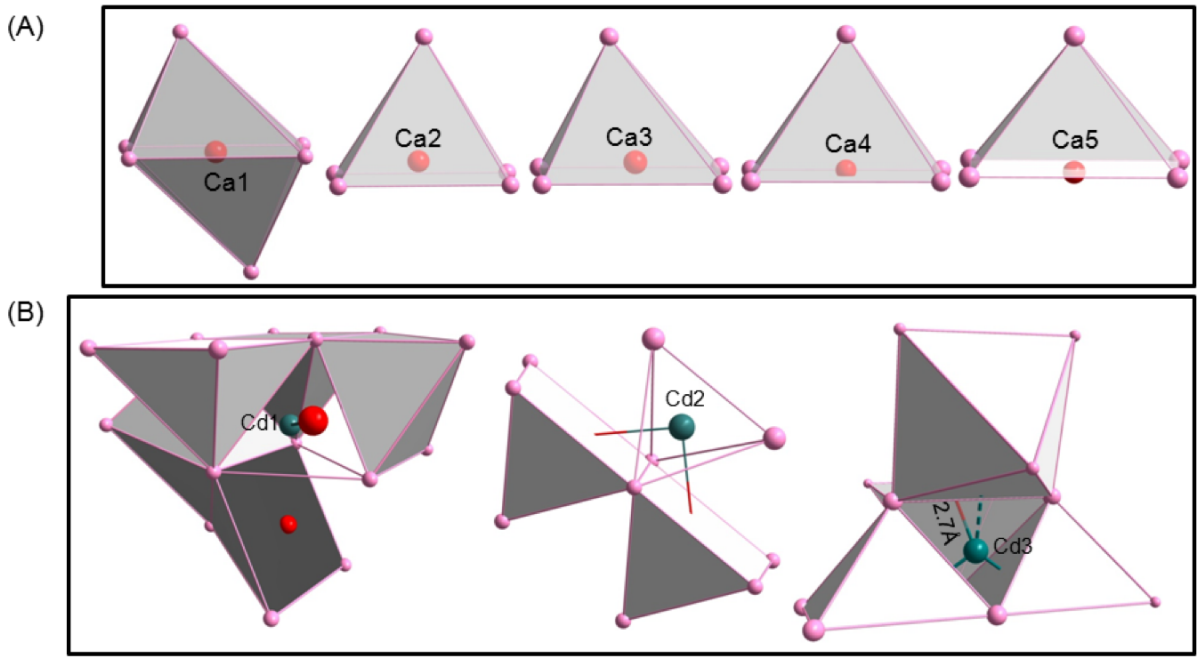

Figure S4. (A) First coordination sphere polyhedra of the Ca atoms in the crystal structure of $Ca_9Cd_{4+x}Bi_9$. The data used for the drawing are from S. Q. Xia and S. Bobev, *J. Am. Chem. Soc.*, 2007, **129**, 10011. (B) $[CdBi_4]$ tetrahedra sharing face and edges with distorted $[CaBi_6]$ octahedra and $[CaBi_5]$ square pyramids.

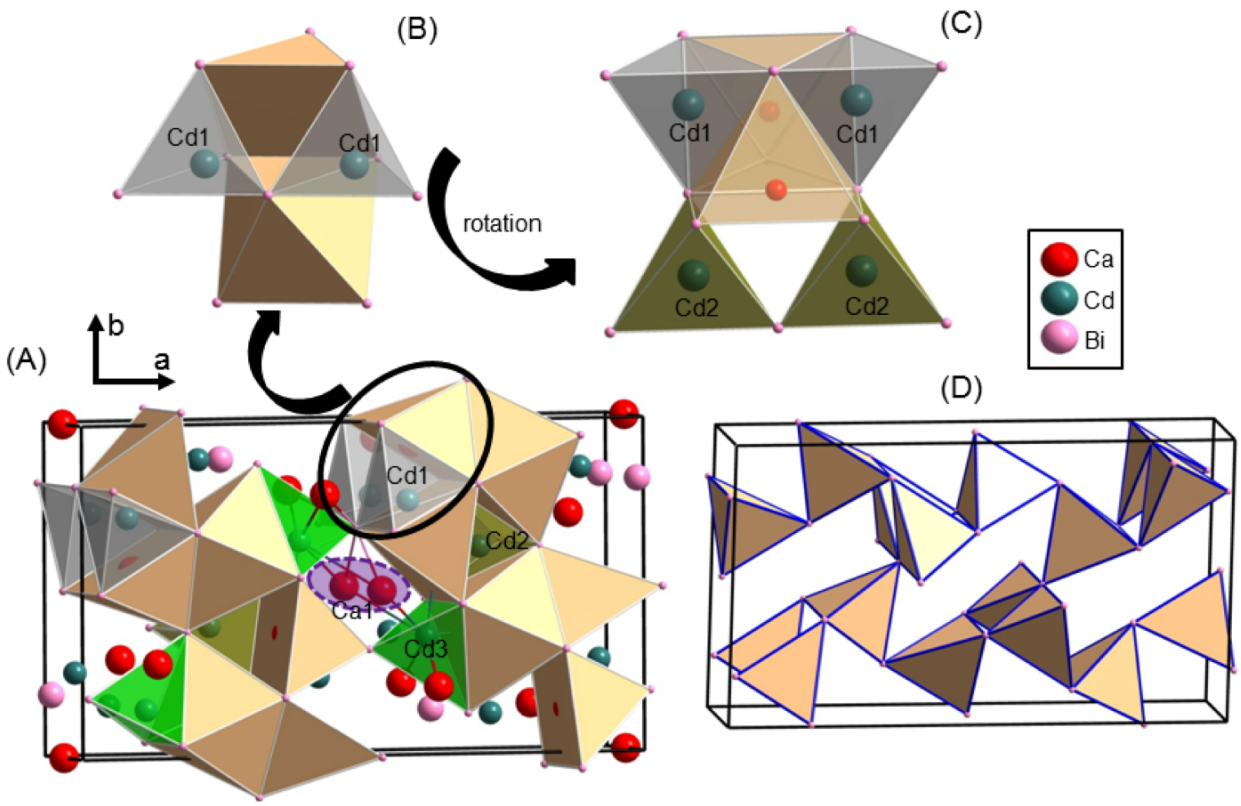

Figure S5. (A) Alternative description of the crystal structure of $Ca_9Cd_{4+x}Bi_9$, viewed as space filling packing of distorted [$CaBi_6$] octahedra and [$CaBi_5$] square pyramids. The Cd atoms occupy the interstitial sites forming a network of distorted [$CdBi_4$] tetrahedra. Each [$CdBi_4$] tetrahedron shares faces and edges with distorted [$CaBi_6$] octahedra and [$CaBi_5$] square pyramids generating surprising robust Cd–Ca bonds. The Ca atoms highlighted in this figure are solely used to fill the space since they are not atoms of the first coordination sphere of Cd3 polyhedron. Note that the remaining Cd and Ca polyhedra and their connectivity are not shown for the sake of clarity. (B) Highlight of the remaining residual space in the crystal structure. This empty space offers more structural flexibility to accommodate diverse cation species with perhaps a new structural topology or stuffed variant. (C) Covalent polyanionic ribbon $[Cd_4Bi_9]^{19-}$ emphasizing the contribution of the electropositive Ca^{2+} unjustly considered as space-filler/spectator. (D) Network of distorted [$CdBi_4$] tetrahedra.